Proceedings of the 28th IEEE
EMBS Annual International Conference
New York City, USA, Aug 30-Sept 3, 2006

Automatic Registration of CT Volumes and Dual-Energy Digital Radiography for Detection of Cardiac and Lung Diseases

Baowei Fei, Xiang Chen, Hesheng Wang, John M. Sabol, Elena DuPont, Robert C. Gilkeson

Abstract—**We are investigating image processing and analysis techniques to improve the ability of dual-energy digital radiography (DR) for the detection of cardiac calcification. Computed tomography (CT) is an established tool for the diagnosis of coronary artery diseases. Dual-energy digital radiography could be a cost-effective alternative. In this study, we use three-dimensional (3D) CT images as the "gold standard" to evaluate the DR X-ray images for calcification detection. To this purpose, we developed an automatic registration method for 3D CT volumes and two-dimensional (2D) X-ray images. We call this 3D-to-2D registration. We first use a 3D CT image volume to simulate X-ray projection images and then register them with X-ray images. The registered CT projection images are then used to aid the interpretation dual-energy X-ray images for the detection of cardiac calcification. We acquired both CT and X-ray images from patients with coronary artery diseases. Experimental results show that the 3D-to-2D registration is accurate and useful for this new application.**

I. Introduction

Cardiovascular disease is the leading cause of death in the United States, responsible for approximately 500,000 deaths per year [1]. More than one millions Americans have heart attacks or angina every year. The increasing incidence of cardiovascular disease makes accurate and noninvasive imaging of early cardiovascular disease increasingly important.

The relationship between coronary artery calcification and atherosclerotic heart disease has been well established [2]. A large body of literature about the detection of cardiac calcification with standard film-screen technology and fluoroscopic techniques exists. Although those techniques have high positive predictive values for the detection of calcium, they have limited sensitivity for the detection of coronary artery disease [3]. The enhanced capabilities of electron beam computed tomography (EBCT) and, more recently, of multi-detector computed tomography (MDCT) to detect coronary calcium have established these techniques as potential screening tools for coronary artery disease [4]. Although these sophisticated techniques have shown considerable promise in the evaluation of coronary artery disease in high-risk populations, whether screening the general population with these advanced techniques will be cost-effective is still unclear.

Recently, digital radiography (DR) has markedly improved imaging of cardiothoracic disease [5]. Digital technology has enabled the use of dual-energy techniques in digital radiography systems. With recently advancements in digital radiography and flat-panel technology, dual-energy subtraction techniques can produce a conventional high-peak-kilovoltage (kVp) image and a low-peak-kVp image with a less than 200-msec temporal separation. Post-processing of these two images results in the following images: a standard image (high kVp image), a subtracted soft-tissues image that removes bone contrast from the underlying lung and mediastinum soft tissue contrast, and a bone image that displays bone and calcified thoracic structure [6]. The detection of calcified cardiothoracic structures is improved on low-energy bone images [7]. In addition to being helpful in the detection of valvular and myocardial calcification, the subtracted bone image is particularly useful in the detection of coronary artery calcification. Unfortunately, standard radiographic images lack 3D spatial information that is important for accurate localization of lesions.

In order to evaluate the ability of digital radiography with dual-energy subtraction for the detection of cardiac calcification, we use three-dimensional (3D) MDCT images as the "gold standard". We propose a 3D-to-2D registration scheme for CT image volumes and dual-energy X-ray images. We first use a 3D CT volume to generate digitally reconstructed radiographs (DRRs) and then register them with dual-energy X-ray images. We call this 3D-to-2D registration. The goal is to fuse the CT projection images with the corresponding X-ray images and thus to aid the interpretation the X-ray images for the localization and detection of calcium.

3D-to-2D registration techniques have been applied to image-guided surgery and image-guided radiotherapy [8-14]. First, DRR images are generated from a 3D CT volume. A variety of methods, such as ray casting, light field, or shear-warp rendering, progressive attenuation fields, and wobbled splatting, are used [15,16].

Second, the 3D model from CT images is rotated and

Manuscript received April 03, 2006. This algorithm developed in this research was partially supported by the NIH grant R21CA120536 and the Case Comprehensive Cancer Center Pilot Award.

B.Fei is with the Departments of Radiology and Biomedical Engineering at Case Western Reserve University, Cleveland, OH 44106, USA (216-844-5281; Fax: 216-844-3106; e-mail: baowei.fei@case.edu).

X.Chen is with the Case Western Reserve University and Xi'an Jiaotong University. H.Wang is with the Department of Biomedical Engineering at Case Western Reserve University. J.M.Sabol is with GE Medical Systems, Applied Science Lab, P.O.Box 414, W-657, Milwaukee, WI 53201. E.DuPont and R.C.Gilkeson is with the Department of Radiology at the University Hospitals of Cleveland, OH 44106, USA.

translated until the DRR image is aligned with the X-ray image. Registration techniques can be generally categorized as feature-based and intensity-based methods. Feature-based methods extract local image features from the 2D and 3D data sets and then transform the model to align the features. Intensity-based methods compare the voxel and pixel values directly using a measure based on image statistics. Different similarity measures and optimization strategies are used for the 3D-to-2D registration [12].

In this paper, we apply intensity-based registration methods to this new application in the detection of coronary artery disease. To the best of our knowledge, there is no report on 3D-to-2D registration of CT volumes and dual-energy X-ray images of the heart. In this study, we reported an automatic registration scheme for this particular application. Both CT and X-ray images were acquired from patients with cardiovascular disease. Experimental results, discussions, and conclusions are also reported.

II. Materials and Methods

A. Image Acquisitions

We originally identified a group of 42 patients with findings suspicious for cardiac calcification on the dual-energy subtracted bone images. In this initial population of 42 subjects, 33 patients have also undergone MDCT evaluation of the chest within 6 months of chest radiography. Six patients with coronary artery diseases were selected for the registration experiments.

Patients were imaged using a digital radiography unit (Revolution XR/d, GE Healthcare). With dual-energy subtraction, a 60-kVp image (low-energy image) was taken. After a 150-msec delay, a second conventional 120-kVp image (high-energy image) was obtained. After post-processing of the two images, a standard 120-kVp image, a subtracted soft-tissue image, and a subtracted bone image were presented. Hard- and soft-copy images were available for review, and images were evaluated by two dedicated chest radiologists. The standard posterior-anterior and lateral radiographs were interpreted first followed by analysis of the subtracted soft-tissue and bone images.

All CT scans were non-ECG gated studies using 4- or 16-slice MDCT. The CT examinations were obtained for a variety of clinical indications using imaging protocols that varied considerably in slice thickness, radiographic technique, and presence or absence of intravenous (IV) contrast material. The CT studies were analyzed for the presence of coronary artery, valvular, or myocardial calcification. These 33 patients undergoing both dual-energy subtraction digital radiography and chest CT were then selected for image analysis. The study group consisted of 14 women and 19 men who ranged in age from 40 to 92 years. The patients had undergone chest radiography for a variety of reasons including preoperative surgical evaluation, pneumonia, and chest pain.

B. Production of DRR Images

We use a shear-warp factorization method to generate DRR images. In this method, a viewing transformation is applied to simplify the projection processing. First, the algorithm uses a principal viewing axis to choose a set of CT voxel slices to resample and composite. Second, it determines the order of the slices along the front-to-back traversal of the volume. Generally, a perspective viewing transformation matrix includes a permutation, a shift of the origin, a 3D perspective shear scale, and a 2D warp [17]. The warp transformation is the product of the view transformation matrix and the inverse of the shear transformation matrix.

The DRR images are simulated using the parameters that were used for real X-ray image acquisitions. The distance between the X-ray source and the detector plane is 1,821 mm. The patient stands as close as possible to the detector plane (less than 50-mm). The DRR images are generated by averaging the CT values of the voxels that intersect with the stimulated casting X-ray. Although all patients were positioned in an approximately posterior-anterior (PA) orientation, patient positioning could slightly vary among patients. To simulate this situation, we generate 21 DRRs images at different angles (±10 degrees) that are centered at the PA direction.

C. Image Registration

We will register the DRR images with the corresponding dual-energy X-ray image. We use normalized mutual information (NMI) as the similarity measure because it has been reported as a robust similarity for many applications [18-21] and because it does not assume a linear relationship between the gray values of two images.

The image registration is performed to align the DRR image to the dual-energy X-ray image. Transforming the DRR image (two translations and one rotation), the algorithm automatically maximizes the NMI between the DRR and X-ray image. We use the downhill simplex method of Nelder and Mead as the search strategy [23]. Optimization of registration ends either when the maximum number of NMI calculations is reached (typically 500) or the fractional change in NMI is smaller than a tolerance (typically 0.0001). We use IDL (Interactive Data Language, Research System Inc., Boulder, CO) as the program language.

For each patient, we register each of the 21 DRR images to the low-energy bone image. As noted earlier, each DRR image was obtained at a different angle. We compare the final NMI values among the 21 DRR images. We select the one with the maximum NMI value as the optimal DRR image that best match the dual-energy X-ray image.

Several preprocessing of the images have been done before registration. X-ray images have been downsampled to 512x512 to improve the speed of registration. The DRR images have the same pixel number and resolution as down-

sampled X-ray images. During the CT image acquisition, the two arms are at the patient's sides. However, the arms are raised to lift the clavicles and scapular so that they are minimally projected onto the lungs. In order to improve registration, the clavicle and scapula have been cropped from X-ray and DRR images to minimize the difference on both images.

The registration was first evaluated by visual comparison. Overlay displays were used to examine structural overlap. One image was rendered in gray, the other in red, and it was quite useful to interactively change the contribution of each image using the transparency scale. We also use difference images and checkerboard display for the evaluation. NMI values were used to quantitatively evaluate the improvement after registration.

III. Materials and Methods

A. CT Projection Images

In Figure 1a-c, 3D volume rendering of the heart from the CT image volume shows extensive calcium deposits within the left coronary arteries (Figure 1a-b) and the aortic valve (Figure 1c). The projection images from the average projection method (Figure 1d-f) also show the calcium.

In Figure 1g-i, the dual-energy X-ray images show findings suspicious for coronary artery calcification that was verified by the CT images. The low-energy bone images (Figure 1g-i) are superior to the standard high-peak kilo-voltage images and the subtracted soft-tissue images (not shown) for the detection of calcium.

The CT projection images are quite useful to aid the interpretation of the dual-energy X-ray images for the detection of calcification. For example, Figure 1f better shows the coronary artery calcium than Figure 1i. Furthermore, the 3D volume rendering images such as Figure 1a-c verified the location of the calcium.

B. Registration Results

We visually evaluate the registration quality of the CT projection images and the dual-energy X-ray images. Before registration, checkerboard images show the misalignment of the bones and other tissues. After registration, the mismatches are corrected in the transformed image.

We also quantitatively evaluate the improvement of the alignment by registration. The NMI values between the CT projection images and the X-ray images were calculated before and after registration. For all the six registration experiments, NMI values always increase after registration. For the 21 different CT projection images that were performed at different angles for each case, the NMI value reaches the maximum when the projection was taken approximately in the posterior-anterior direction. This is because the dual-energy X-ray images were acquired in this direction. For the six experiments, they are located at 3, 1, 1, -1, 2, and 5 degrees, respectively. For these optimal projections images, the NMI values increase from 0.10±0.02 before registration to 0.13±0.01 after registration.

IV. Discussion and Conclusion

We developed an image processing and analysis approach including projection and registration for dual-energy digital radiography and CT volume images for the detection of cardiac calcification. Three-dimensional CT image data including volume rendering and projection images were used to aid the interpretation of digital radiography. An automatic registration for 3D CT volumes and 2D dual-energy X-ray images was developed and evaluated. This 3D-to-2D registration algorithm may provide a useful tool for the new application in dual-energy digital radiography for the detection of cardiac calcification.

References

[1] B.H.Thompson and W.Stanford, "Imaging of coronary calcification by computed tomography," J.Magn Reson.Imaging, vol. 19, pp. 720-733, Jun, 2004.

[2] L.Wexler, B.Brundage, J.Crouse, R.Detrano, V.Fuster, J.Maddahi, J.Rumberger, W.Stanford, R.White, and K.Taubert, "Coronary artery calcification: pathophysiology, epidemiology, imaging methods, and clinical implications. A statement for health professionals from the American Heart Association. Writing Group," Circulation, vol. 94, pp. 1175-1192, Sep 1, 1996.

[3] C.P.Heussel, T.Voigtlaender, H.Kauczor, M.Braun, J.Meyer, and M.Thelen, "Detection of coronary artery calcifications predicting coronary heart disease: comparison of fluoroscopy and spiral CT," Eur.Radiol., vol. 8, pp. 1016-1024, 1998.

[4] B.H.Thompson and W.Stanford, "Update on using coronary calcium screening by computed tomography to measure risk for coronary heart disease," Int.J.Cardiovasc.Imaging, vol. 21, pp. 39-53, Feb, 2005.

[5] C.Schaefer-Prokop, M.Uffmann, E.Eisenhuber, and M.Prokop, "Digital radiography of the chest: detector techniques and performance parameters," J.Thorac.Imaging, vol. 18, pp. 124-137, Jul, 2003.

[6] H.MacMahon, "Digital chest radiography: practical issues," J.Thorac.Imaging, vol. 18, pp. 138-147, 2003.

[7] R.C.Gilkeson, R.D.Novak, and P.Sachs, "Digital radiography with dual-energy subtraction: improved evaluation of cardiac calcification," AJR Am.J.Roentgenol., vol. 183, pp. 1233-1238, Nov, 2004.

[8] J.Kim, F.F.Yin, Y.Zhao, and J.H.Kim, "Effects of x-ray and CT image enhancements on the robustness and accuracy of a rigid 3D/2D image registration," Med.Phys., vol. 32, pp. 866-873, Apr, 2005.

[9] J.H.Hipwell, G.P.Penney, R.A.McLaughlin, K.Rhode, P.Summers, T.C.Cox, J.V.Byrne, J.A.Noble, and D.J.Hawkes, "Intensity-based 2-D-3-D registration of cerebral angiograms," IEEE Trans.Med.Imaging, vol. 22, pp. 1417-1426, Nov, 2003.

[10] J.Weese, G.P.Penney, P.Desmedt, T.M.Buzug, D.L.Hill, and D.J.Hawkes, "Voxel-based 2-D/3-D registration of fluoroscopy images and CT scans for image-guided surgery," IEEE Trans.Inf.Technol.Biomed., vol. 1, pp. 284-293, Dec, 1997.

[11] D.B.Russakoff, T.Rohlfing, K.Mori, D.Rueckert, A.Ho, J.R.Adler, Jr., and C.R.Maurer, Jr., "Fast generation of digitally reconstructed radiographs using attenuation fields with application to 2D-3D image registration," IEEE Trans.Med.Imaging, vol. 24, pp. 1441-1454, Nov, 2005.

[12] G.P.Penney, J.Weese, J.A.Little, P.Desmedt, D.L.Hill, and D.J.Hawkes, "A comparison of similarity measures for use in 2-D-3-D medical image registration," IEEE Trans.Med.Imaging, vol. 17, pp. 586-595, Aug, 1998.

[13] R.A.McLaughlin, J.Hipwell, D.J.Hawkes, J.A.Noble, J.V.Byrne, and T.C.Cox, "A comparison of a similarity-based and a feature-based 2-D-3-D registration method for neurointerventional use," IEEE Trans.Med.Imaging, vol. 24, pp. 1058-1066, Aug, 2005.

[14] G.P.Penney, P.G.Batchelor, D.L.Hill, D.J.Hawkes, and J.Weese, "Validation of a two- to three-dimensional registration algorithm for aligning preoperative CT images and intraoperative fluoroscopy images," Med.Phys., vol. 28, pp. 1024-1032, Jun, 2001.
[15] T.Rohlfing, D.B.Russakoff, J.Denzler, K.Mori, and C.R.Maurer, Jr., "Progressive attenuation fields: fast 2D-3D image registration without precomputation," Med.Phys., vol. 32, pp. 2870-2880, Sep, 2005.
[16] W.Birkfellner, R.Seemann, M.Figl, J.Hummel, C.Ede, P.Homolka, X.Yang, P.Niederer, and H.Bergmann, "Wobbled splatting--a fast perspective volume rendering method for simulation of x-ray images from CT," Phys.Med.Biol., vol. 50, pp. N73-N84May 7, 2005.
[17] P.G.Lacroute, Fast Volume Rendering Using A Shear-Warp Factorization Of The Viewing Transformation Anonymous Technical Report: CSL-TR- 95-678, 1995. Stanford University - Computer Systems Laboratory of Departments of Electrical Engineering and Computer Science. Stanford, CA.
[18] J.P.Pluim, J.B.Maintz, and M.A.Viergever, "Mutual-information-based registration of medical images: a survey," IEEE Trans.Med.Imaging, vol. 22, pp. 986-1004, Aug, 2003.
[19] B.Fei, J.L.Duerk, D.T.Boll, J.S.Lewin, and D.L.Wilson, "Slice-to-volume registration and its potential application to interventional MRI-guided radio-frequency thermal ablation of prostate cancer," IEEE Trans.Med.Imaging, vol. 22, pp. 515-525, Apr, 2003.
[20] B.Fei, A.Wheaton, Z.Lee, J.L.Duerk, and D.L.Wilson, "Automatic MR volume registration and its evaluation for the pelvis and prostate," Phys.Med.Biol., vol. 47, pp. 823-838, Mar 7, 2002.
[21] B.Fei, J.L.Duerk, and D.L.Wilson, "Automatic 3D registration for interventional MRI-guided treatment of prostate cancer," Comput.Aided Surg., vol. 7, pp. 257-267, 2002.
[22] F.Maes, A.Collignon, D.Vandermeulen, G.Marchal, and P.Suetens, "Multimodality image registration by maximization of mutual information," IEEE Trans.Med.Imaging, vol. 16, pp. 187-198, Apr, 1997.
[23] J.Nelder and R.A.Mead, "A simplex method for function minimization," Computer Journal, vol. 7, pp. 308-313, 1965.

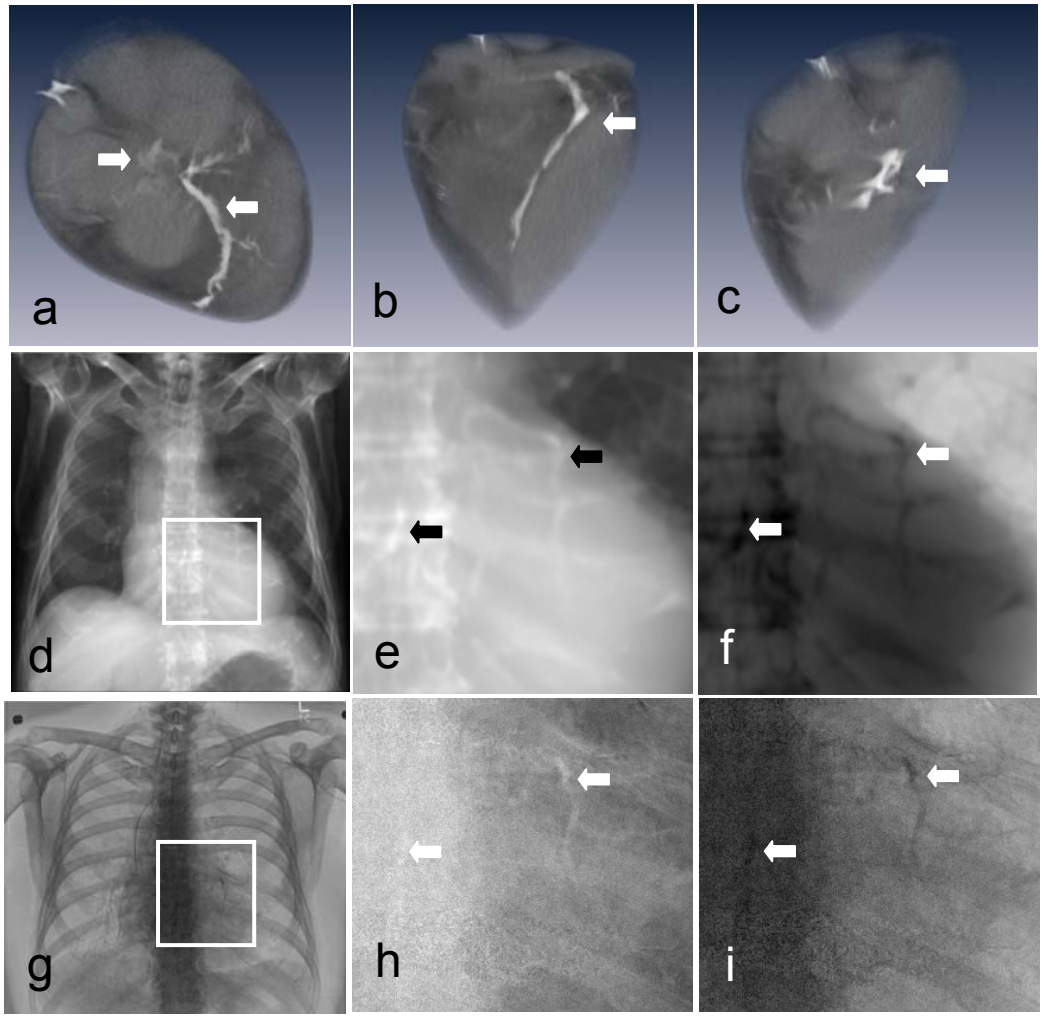

Figure 1. CT and dual-energy X-ray images for calcium. *Top*: Three-dimensional (3D) volume rendering of the heart from the CT image volume that show extensive calcium deposits within the left coronary arteries (arrows in a and b) and the aortic valve (arrow in c). *Middle:* CT projection images using the average intensity method. The rectangular region on the right image is magnified and shown at the center and right. Image on the right is the inverse of the central image. Arrows indicate the calcium. *Bottom:* Dual-energy bone images that display bones and calcified structures (arrows).